Civil Engineering and Architecture 13(6): 4450-4461, 2025 http://www.hrpub.org
DOI: 10.13189/cea.2025.130624

Experimental Investigation of Bond Strength of Concrete with Glass Fiber Reinforced Polymer Bar under Static Loading Condition Using Pull-out Testing

Ariane T. Lacson, Darren Russel D. Tanay, Pia Abigail P. Torres, Gilford B. Estores*

School of Civil, Environmental, and Geological Engineering, Mapua University, Philippines

Received March 26, 2025; Revised September 12, 2025; Accepted October 22, 2025

Cite This Paper in the Following Citation Styles

(a): *[1] Ariane T. Lacson, Darren Russel D. Tanay, Pia Abigail P. Torres, Gilford B. Estores , "Experimental Investigation of Bond Strength of Concrete with Glass Fiber Reinforced Polymer Bar under Static Loading Condition Using Pull-out Testing," Civil Engineering and Architecture, Vol. 13, No. 6, pp. 4450 - 4461, 2025. DOI: 10.13189/cea.2025.130624.*

(b): *Ariane T. Lacson, Darren Russel D. Tanay, Pia Abigail P. Torres, Gilford B. Estores (2025). Experimental Investigation of Bond Strength of Concrete with Glass Fiber Reinforced Polymer Bar under Static Loading Condition Using Pull-out Testing. Civil Engineering and Architecture, 13(6), 4450 - 4461. DOI: 10.13189/cea.2025.130624.*

Abstract The bond strength between Glass Fiber Reinforced Polymer (GFRP) bars and concrete is a critical factor in determining the ability and effectiveness of this alternative reinforced material compared to traditional steel reinforcement in structural applications, especially under static loading conditions. Despite the increasing use of GFRP bars due to their physical property, corrosion resistance, high tensile strength, and lightweight nature, there is a notable lack of research studies addressing their bond behavior with concrete under static loading. This study aims to focus on filling this gap by investigating the bond strength and the factors affecting the bond between GFRP bars and concrete. The study employs pull-out testing that applies gradual increases in loading to know how GFRP bars behave under this testing. It was compared to traditional reinforcement to know if it can be used as an alternative reinforcement in structures that require crucial bond strength. The findings revealed that GFRP bars exhibit lower bond strength than steel, with an observed reduction of about 17.404%. Additionally, an inverse relationship between bar diameter and bond strength was identified. The results provide valuable insights into the performance of GFRP reinforcement, highlighting its benefits and limitations, and supporting its potential use in concrete structures.

Keywords Bond Strength, Reinforced Concrete, Concrete, Glass-Fiber Reinforced Polymer Rebar, Uncoated Reinforcement, Static Loading, Pull-out Testing

1. Introduction

The dynamics of bond behavior between a reinforcement bar and concrete are crucial in establishing and maintaining the integrity of a reinforced structural element, as their relationship starts when the two materials are joined together as the concrete toughens. A significant amount of force is required to pull out a bar when it is implanted within concrete. The capacity to resist to making it slip out of the bonding interaction is called Bond Strength. That said, it directly affects a member's crack resilience and load-carrying capacity, and the lack thereof may lead to structural failure.

The interdependence of concrete and reinforcement is due to the give-and-take relationship between the two materials, whereas the tensile fragility of concrete is compensated by the bars by about 100 times. Due to this, the two will work together and resist the slippage of one another, attaining a high bond strength [1]. Furthermore, stirrup confinement enhances the bond performance of structural elements. It acts as a lateral support to prevent the concrete from disintegrating when the bond weakens [2].

While concrete effectively acts as a protective barrier against the penetration of corrosive agents in reinforced structures primarily due to its highly alkaline nature, it is essential to acknowledge that cracks may inevitably develop over time due to environmental factors. In this instance, the bar area is expanded, reducing the cross-section. Thus, its allotted space in the concrete and strength were disturbed, causing it to experience tension stress and, later, cracking and, worse, splitting. Therefore, theoretically, ultimate bond strength depends on corrosion values, whereas the higher the corrosion, the lower the bond strength [3]. To appease the problem, studies explored various parameters wherein the utilization of Fiber-Reinforced Plastics (FRP) as a substitute for conventional steel rebar stood out due to its lightweight material, high tensile strength, and non-corrosiveness.

Furthermore, the feasibility of GFRP rebar as a replacement for typical steel rebars in constructing different structures made of concrete has been verified [4]. It is noted that GFRP composite, as being combined with coarse ingredients, can be subject to factors of increasing a bond strength occurring between the rebar and concrete itself. The GFRP rebar resulted in a higher yield strength than the typical steel rebar but with higher yield strain too. This indicates that the GFRP rebar can have a higher tensile strength than the steel rebar.

In terms of the compressive and flexural strength, the GFRP rebars were found to be acceptable as per the specifications of the British Standard to be used for RC structures. This proves that GFRP rebars are a decent replacement for steel rebars for building structures. Aside from being advanced, this type of rebar is non-corrosive which means that it has an advantage in harsh environments where the traditional reinforcement like steel is vulnerable. The maintenance of GFRP rebars can be beneficial economically in terms of costs since the lifespan is longer. Thus, this can also produce reinforced concrete beams with high properties like the bond strength, which is vital since RC beams are prone to being subjected to different types of loads [4].

Figure 1 illustrates the difference between steel reinforcement bars (SRB), which are traditionally used in the Philippines, and glass fiber reinforced bars (GFRB). Notable differences can be observed between these two types of reinforcement. Both reinforcements have ribbed patterns to enhance bonding with concrete, but the ribs on GFRB are more uniform and slightly rounded compared to SRB. Furthermore, the material composition of the two bars differs significantly, with SRBs being metallic and prone to corrosion, whereas GFRBs are made of composite materials, offering corrosion resistance. Although not directly visible in the image, GFRBs are also considerably lighter than SRBs due to their fiberglass composition, which can influence handling and structural performance.

(a) (b)

Figure 1. (a) SRB ; (b) GFRB

Nowadays, various methods are being studied and applied to enhance the reinforcement's performance, including coating to prevent corrosion. However, the uncoated reinforcement is still being employed because of its ductility, cost-effectiveness, and still high tensile strength. Additionally, it was found that when the concrete experienced splitting failure, the bond strength of epoxy-coated bars was reduced by 18% compared to uncoated bars [5].

In addition, the bond strength of textured-coated reinforcement was up to 19% lower than the uncoated bars [6]. This textured coating did not provide additional improvement in post-peak bond-slip behavior, which suggests that even if texture has the ability to enhance the bond, the coating did not effectively compensate for the reduction in bond strength.

In a recent study, static load is defined as a weight that remains stationary for a significant duration without any movement or change in stance. Hence, it is used in testing, whereas controlled external loads were needed to evaluate concrete specimens [7]. Utilizing static loading exhibited limited stiffness and deflection of a beam to analyze if the sample would be more endurable when bonded with steel plates [8]. Nonetheless, the damage degree of different concrete sampling can be evaluated with Dynamic and Static Loading to open the variation of sample analysis [9]. Additionally, there are the advantages of using a hybrid fiber system to heighten the ultimate limit state (ULS) cracking performance of reinforced concrete beams [10]. In doing so, the investigation placed the samples under consistent loading conditions throughout the 28-day curation period. Relatively, in the Declaration of Performance (DOP) of anchoring mortars for reinforcement to meet the requirements of the harmonized standard (hEN) EN 1504-6 (EN 1504-6, 2006), static loading was applied to ensure that the execution of the test had been evaluated according to the requirements in the known provision as per European Standards. It asserted that non-static loading could not accurately predict the damage to the specimen under its gradual collapse [11]. Thus, the study urged employing static loading to achieve more reliable results in understanding the behavioral dynamics of samples under different loads. This study can potentially promote wider adoption of glass rebar as an alternative to other reinforcement like traditional steel reinforcement. With the properties that the GFRP has, this study will also contribute to the development of more reliable infrastructures, especially when bond performance is understood; there will be a high tendency that material usage will be reduced, which will enhance the quality of the structures without compromising its cost

2. Materials and Methods

2.1. Data Gathering Instruments

2.1.1. Specimen Preparation

The specimens used in this study were prepared in accordance with ASTM C31/C31M-22. This standard provided clear guidelines for mixing, casting, and curing of specimen samples in this experiment, ensuring consistency throughout the process. Since workability is one of the characteristics of a desirable concrete mix design, the researchers followed the ratio of 1:2:4, having 1 part of cement, 2 parts of sand, and 4 parts of gravel. This standard allowed the specimen to have a characteristic compressive strength of 20 MPa or 2900 psi after 28 days of curing.

2.1.2. Glass Fiber Reinforced Polymer (GFRP) and Steel Reinforcement Bars

The GFRP used in this study was supplied by Armastek Philippines - Mahanaim Consulting and Development Inc. They have a diameter of 8 mm and 12 mm which are equivalent to 12 mm and 16 mm steel reinforcement, respectively in terms of tensile strength. This reinforcement passed the fire test and has an average tensile strength of 1200 MPa. However, according to Armastek Philippines, the bond strength of this rebar is not yet tested. And as shown in Figure 1, the reinforcements were marked to identify the contact area when they were cast and tested.

2.1.3. Concrete

The cement used was bought from a hardware store. It was used in reinforced concrete and underwent a sieving process first. Then, the cement was stored until the other materials were ready for the experiment. Tap water was also used to test the specimen. The aggregates used were common crushed stones having a distinct maximum size.

2.2. Concrete Mixing

Concrete mix is a critical phase in this process, and achieving the concrete grade of M20 involves careful consideration of mix proportions. In this study, the specified concrete mix design entails a combination of cement, fine aggregate, and coarse aggregate, adhering to a ratio of 1:2:4, respectively. These concrete ingredients were mixed thoroughly until water was ready to be added. The process of concrete mixing was used repeatedly until all the concrete molds were prepared.

2.3. Slump Testing

The slump testing was done right after obtaining the proper concrete mix. This test was conducted using a slump cone, having dimensions of 4 inches by 8 inches by 12 inches. It was positioned on a flat surface and filled with three layers, with each layer being tamped 25 times using a tamping rod (ASTM C143/C143M-12). After the last tamping, the excess concrete mix was screeded off, and the concrete around the base of the cone was wiped away. Subsequently, the slump of the concrete was determined by measuring the vertical displacement from the top of the mold to the initial center position of the concrete before any disturbance. The result provided one of the following: True, Zero, Collapse, or Shear slump.

2.4. Casting of Concrete and Installation of Reinforcement Bars

After passing the slump test and achieving the right concrete mix design, the mixture was cast in cylindrical molds following the requirements of ASTM C470/C470M-12. The samples were divided into four groups, with each group containing five samples for data accuracy. The first group had a glass fiber reinforcement bar with a diameter of 8 mm. The second group consisted of steel samples with a 12 mm diameter, as this steel diameter is equivalent to the 8 mm glass bars. The third group sample had a glass fiber reinforcement bar with a diameter of 12mm. Finally, the last group contained steel reinforcement with a diameter of 16 mm, which is equivalent to the glass diameter of the third group sample.

As shown in Figure 2, each group was cast in 150 mm x 300 mm PVC cylinder molds. This was done by placing the reinforcement and curing the mixture by pouring the vessel or using a shovel to transfer the mixture from the batching pan to the molds (Lamb, n.d.). Likewise, each layer was tamped 25 times to ensure there were no voids. These steps were repeated until all 20 specimen samples were prepared.

(a) (b)

Figure 2. Cylinder molds: (a) casting of concrete on PVC; (b) casting of reinforcement

2.5. Curing of Concrete

The specimen samples underwent the process of curing right after casting. Once molded, the specimens were covered and stored for up to 48 hours, following the guidelines of ASTM C31/C31M-22 to preserve the temperature and moisture conditions of the concrete samples. After this period, the specimens were carefully removed from the cylindrical molds and transitioned to the moist curing environment. It was also equipped with water control measures to ensure that the water temperature in the storage remained within the prescribed range. All 20 samples were cured simultaneously for 28 days to achieve their ultimate compressive strength and obtain reliable results (Indian Standard 9103).

2.6. Research Design

The experimental research design was selected as the best approach for this study. The variables in this study suited the approach since these are measurable, step-by-step processes, and objective. Additionally, the outcome of this study was determined upon testing and does not condone subjective conclusions and assumptions. Also, the study was abundant in terms of scientific and engineering concepts that require statistical data and calculations during analysis. The study was also answerable by either true or false on whether there was a bond strength or none. In terms of errors, probable errors were subject to human errors and malfunction of equipment. Thus, the experimental research design was fitted to satisfy all of the objectives of this study.

2.7. Specimen Set-up

In Figure 3, the reinforcement sample having a length of 650 mm was cast in the concrete, where the 150 mm is the embedded length and the remaining 500 mm is the exposed length. The concrete samples have a diameter of 150 mm and a length of 300 mm. Hence, only half of the concrete length has the reinforcement embedded in it.

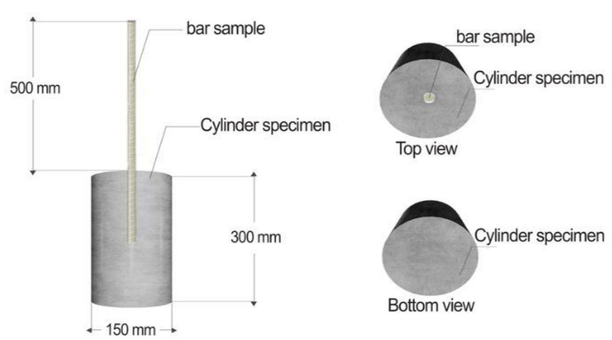

Figure 3. Test Specimen Set-up

Meanwhile, once all the specimens were ready, they underwent pull-out testing using the universal testing machine (UTM). The specimen was placed on the lower steel plate, while the part where the reinforcing bar was exposed was placed in the hole of the plate. The apparatus was attached to the embedded reinforcement, and the instrument allowed the application and gradual increase of static tensile load, as shown in Figure 4. During testing, the data were continuously observed and monitored to gather accurate displacement and failure mode on each RC specimen and to determine the amount of load the specimen experienced before changes occurred. When the testing was completed, the gathered quantitative data and observations were organized and tabulated.

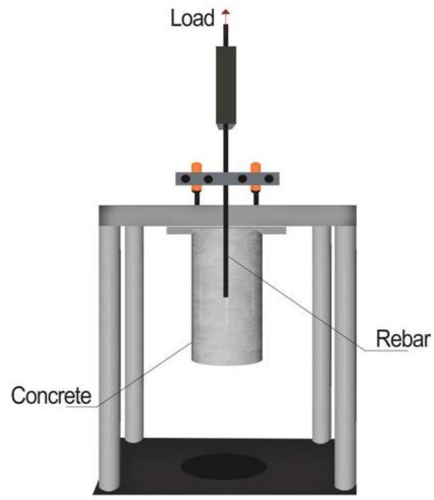

Figure 4. Specimen under Universal Testing Machine

2.8. Methods

In pursuit of interpreting the dataset and understanding the parameters of the research paper, the researchers relied upon the following formula and statistical treatments to calculate various metrics:

2.8.1. Average Bond Strength

As per the American Concrete Institute (ACI) design code, there is an equilibrium of bond stresses holding the reinforcement bar in place within the concrete, as illustrated in Figure 5, considering that the bond stresses along the bond length are under uniform distribution.

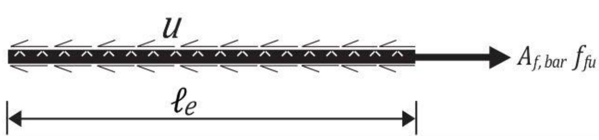

Figure 5. Transfer of Force through Bond

Therefore, from here, the average bond strength between reinforcement bars and concrete is calculated using:

$$\tau=\frac{F_u}{\pi l_e d_b} \tag{1}$$

Where:

τ = is the average bond strength (MPa)
F_u = ultimate pull-out load (kN)
l_e = embedded length (mm)
d_b = diameter of the rebar (mm).

2.8.2. Two-Way Analysis of Variance (ANOVA)

This research study utilized a Two-way Analysis of Variance (ANOVA) to compare 20 specimens. The two types of bars, GFRP and steel bar-induced RC, were placed under two cases with five trials each: 8 mm and 12 mm GFRP bars, respectively, and their 12 mm and 16 mm equivalents in steel bars. The study determined whether the bar sizes and the usage of GFRP and steel bars had a statistically significant effect on bond performance. Two-way ANOVA was chosen as it considered two independent variables and divided the sample into two criteria to explore the bond strength of RC.

That said, the homogeneity of variance was tested through descriptive statistics, where each condition was required to exhibit a specific significance level, expressed as an alpha value of 0.05. Given that the data included two bar sizes and five different sample subjects, this statistical treatment helped in deciding whether to reject or accept the null hypothesis.

Suppose that a total of 20 specimens were arranged into two groups: GFRP-X, GFRP-Y, SB-X, and SB-Y. Given each group's different bar sizes and two different distinctions of rebars, the data would be as shown in Table 1 through the said statistical treatment.

As per the dfA and dfB, n signifies the number of groups per factor, however in terms of the $p-value$, the said equivalents must be looked up in the F-distribution table through the identification of the degree of freedom and $F-value$.

Afterwards, the sum of squares for each (GFRP & Steel) to find the mean for each as well as its total mean is calculated by using the formula SS=(x-x)2. Then, solving for the total sum of squares refers to the application of the Sum of Squares formula with respect to the response variable for all the tests done by using the total mean.

Then calculating for the interaction effect *(SS AB)* comes next through the use of SS $AB = SSTotal - SSA - SSB - SSW$. The degrees of freedom (df) come next as it is the quantity of independent values within the sampling.

- GFRP (dfA) = quantity of total groups in GFRP as reinforcement – 1
- GFRP (dfB) = quantity of total groups in Steel as reinforcement – 1
- Degrees of freedom for the interaction effect (dfI) = $dfA * dfB$
- Degrees of freedom for within (dfW) = the total number of observations - (quantity of groups in GFRP x quantity of groups in steel)
- ($dfTotal$) = the total number of testing – 1

2.8.3. Multiple Regression Analysis

After identifying whether there was a significant difference between the samples, a multiple linear regression analysis further quantified the significance. This analysis demonstrated the relationship trend between the two independent variables: the type of reinforcement bar and bar dimensions, and their impact on overall bond performance. The model utilized the regression line to assess whether a positive or negative relationship existed between the variables and to identify any outliers within the dataset.

Knowing the association of GFRP's bond slip and bond strength to the RC provided insight into theoretical inferences about its performance as reinforcement compared to traditional steel bars.

To analyze the effect of different bar dimensions per sample group (GFRP and Steel) on the bond strength of the RC, multiple regression analysis was used to optimize the gathered data through the equation:

$$Y = \beta_0 + \beta_1 X_1 + \beta_2 X_2 + \beta_3 X_3 + \beta_4 X_4 \quad (2)$$

In the equation depicted, the Y represents the bond strength acquired from the Pull-Out Testing under the ASTM ASTM D7913/D7913M-21 standard. Then, $\beta_1 X_1$ and $\beta_2 X_2$ refer to the two different dimensions of reinforcement bars, denoting the 8 mm and 12 mm GFRP bars, and their 12 mm and 16 mm equivalents in steel bars. It was then followed by the binary variable representing the reinforcement type (1 for GFRP, 0 for Steel), which follows the equation $\beta_3 X_3$ for the GFRP bar while $\beta_4 X_4$, for the steel reinforcement.

Table 1. Two-way Analysis of Variance

Source of Variation	Sum of Squares	Degrees of Freedom	Mean Squares	F-Value	p-value
GFRP	SSA	$dfA = nA - 1$	$MSA = \frac{SSA}{dfA}$	$\frac{MSA}{MSW}$	
Steel bar	SSB	$dfA = nb - 1$	$MSA = \frac{SSA}{dfA}$	$\frac{MSB}{MSW}$	
Interaction effect	SSAB	$dfAB = dfA - dfb$	$MSA = \frac{SSAB}{dfAB}$	$\frac{MSAB}{MSW}$	
Within (error)	SSW	$dfW = N - nA - nB$	$MSW = \frac{SSW}{dfW}$		
Total	SSTotal	$dfTotal = N - 1$			

3. Results and Discussion

3.1. Failure Mode

The failure mode of bond samples between concrete and GFRP bars can be defined using two different types, including splitting failure and pull-out failure. Splitting failure happens when the concrete develops cracks that cause the bond between the concrete and the GFRP bars to break. Usually, a break in the concrete surrounding the rebar results from these cracks, which begin at the area where the rebar and concrete meet and spread outward. On the other hand, pull-out failure happens when the rebar gradually pulls from the concrete without creating visible cracking or splitting. As shown in Figure 6, it can be distinguished relative to its displacement.

In the data gathered shown in Table 2, the GB- 8 group samples were the only variables that failed due to splitting, which can be caused by smaller bar diameter, brittle nature, and a much smoother surface compared to the other bar samples tested, which led into the bond between the bar and reinforcement to create a radial tension causing the bar to pull apart in a perpendicular manner. When tensile stress exceeds the reinforcement itself, the bar splits, which is the case for GB-8 samples, where it occurred prior to its anticipated pull-out failure, which is common in smaller diameter rebars, which lack confinement capability.

(a) (b) (c) (d)

Figure 6. Failure modes: (a) 8mm GFRP bar; (b) 12mm GFRP bar; (c) 12 mm Steel Bar; (d) 16 mm Steel bar

Table 2. Summary of Pull-out test results

Sample No	Fu (kN)	*Fu (kN)	Displacement (mm)	τu (MPa)	*τu (MPa)	Failure Mode
GB 8-1	15.867		-	4.209		S
GB 8-2	13.193		-	4.000		S
GB 8-3	13.585	14.5494	-	3.604	3.9596	S
GB 8-4	15.246		-	4.044		S
GB 8-5	14.856		-	3.941		S
SB 12-1	19.169		20	3.390		P
SB 12-2	28.955		22	5.120		P
SB 12-3	25.685	23.8752	21	4.542	4.2220	P
SB 12-4	23.415		20	4.141		P
SB 12-5	22.152		20	3.917		P
GB 12-1	17.892		7	3.164		P
GB 12-2	13.060		5	2.310		P
GB 12-3	16.288	15.75	7	2.880	2.7852	P
GB 12-4	14.256		5	2.521		P
GB 12-5	17.254		7	3.051		P
SB 16-1	14.422		15	1.913		P
SB 16-2	24.936		16	3.307		P
SB 16-3	19.854	19.9032	15	2.633	2.6398	P
SB 16-4	16.856		15	2.236		P
SB 16-5	23.448		16	3.110		P

F_u *is the ultimate pull out load ;* $*F_u$ *is the average ultimate pull out load;* F_u *is the calculated bond strength;* $*\tau_u$ *is the average bond strength;* ***S*** *is splitting failure; and* ***P*** *is for pull out failure*

3.2. Load-Displacement

Comparing the groups of samples, SB samples generally resulted in a higher Ultimate Load than GB, with SB-12 acquiring the highest average, followed by SB-16, GB-12, and GB-8. It acquired a correlation coefficient of 0.8157, denoting a positive relationship, wherein the displacement increases along with the Ultimate Load. Also, as shown in Figure 7, the distribution trend generally rises, given a higher ultimate load and a corresponding higher displacement.

Consecutively, as shown in Figure 8, the ultimate loads of series 1 varied from 13.19 to 15.87 kN corresponding to the bond strength of 3.604 to 4.209 MPa, which is in series 2. The zero displacement among this group explains its capacity to split even before undergoing the pull-out failure due to high bond stress. Error bars were considered to indicate moderate variability. The graph also points to the premature splitting failure to analyze the limits in bond developments, as the sample lacked displacement compared to the other groups.

With displacement ranging from 20mm to 22mm in Figure 9, the loads plotted in Series 1 rose from 20 kN to 29 kN, with a proportionally increasing bond strength of 3.5 MPa to 5 MPa. With the positive load-bond relationship, the data suggested a steady and strong bond development for series 1. However, series 2 follows the same pattern but at a lower scale. Error bars were included to show variability. However, all samples in this group executed a pull-out failure response, which is commonly anticipated. Overall, the group of 12mm steel bars portrayed an effective bond performance and ductile pull-out behavior, which explains its commercial use.

The 12mm glass bar resulted in a 13 kN to 18 kN ultimate load at 5mm to 7mm displacement, which is considered a low deformation in Figure 10. This corresponds to the bond strength of 2.5 MPa to 3.2 MPa. This group also demonstrated a pull-out failure with moderate bond strength, which improved compared to the data acquired from the 8mm diameter GFRP. Error bars were added to evaluate how narrow and consistent the result is and to show the diameter and its confinement improve the bond behavior between the concrete and the glass rebar.

In Figure 11, the 16mm Steel bar's ultimate load varied from 15 kN to 25 kN at a displacement of 15mm to 16mm, which gave a higher load-bearing capacity as well as its deformation. In line with this, the bond strength of the reinforcement ranged from 2.5 MPa to 3.5 MPa. The trend shows a significant load response for both series. On the other hand, the wide error bars defined more variability, which plots the stable pull-out failure with high load capacity. The graph also highlighted the relationship between the diameter and bond stress to evaluate the upper capacity limit of large diameter rebars like in this group, in terms of embedment and confinement conditions.

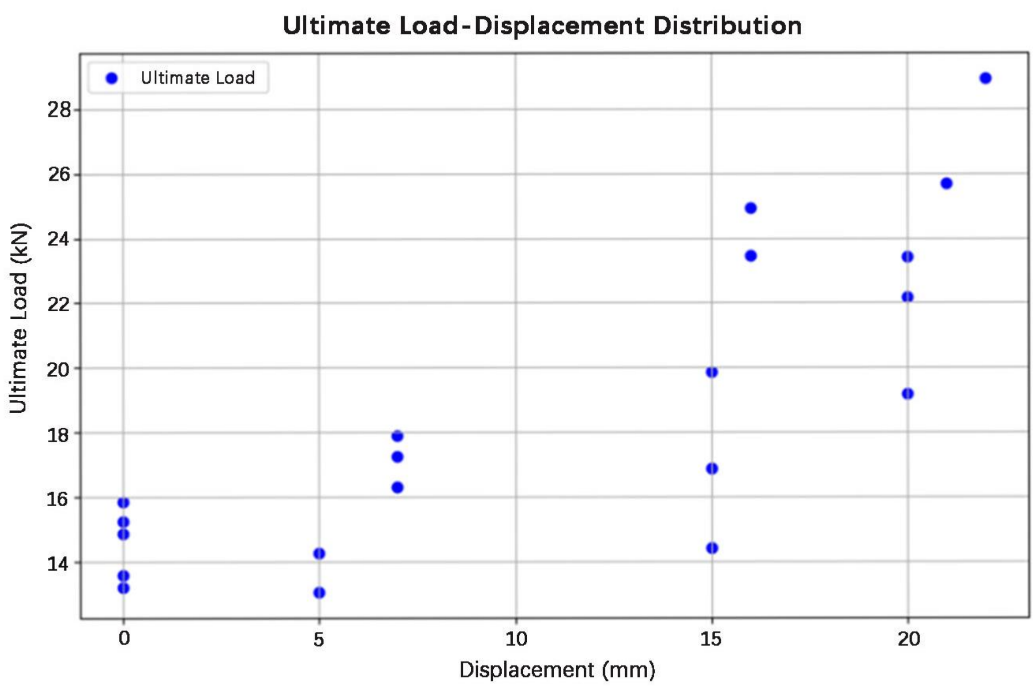

Figure 7. Load-displacement distribution of the samples

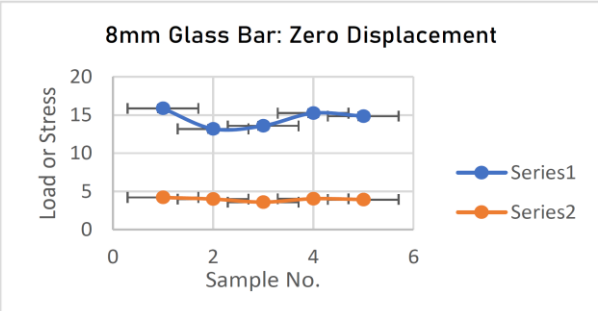

Figure 8. Load distribution at zero displacement curve of 8mm GFRP

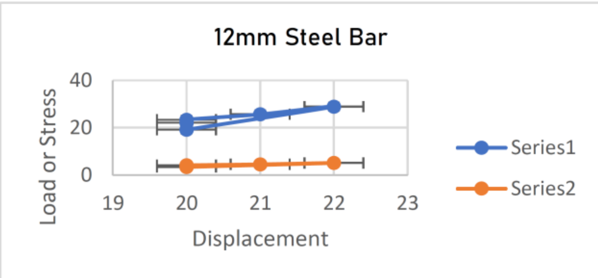

Figure 9. Load-displacement curve of 12mm Steel Bar

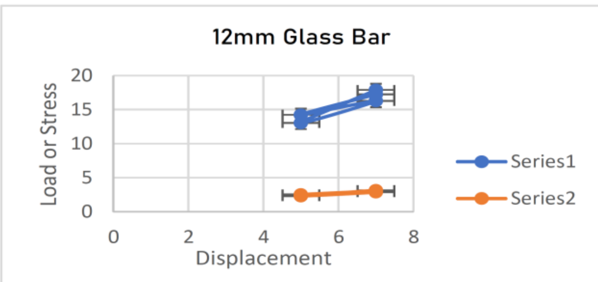

Figure 10. Load-displacement curve of 12mm Glass Bar

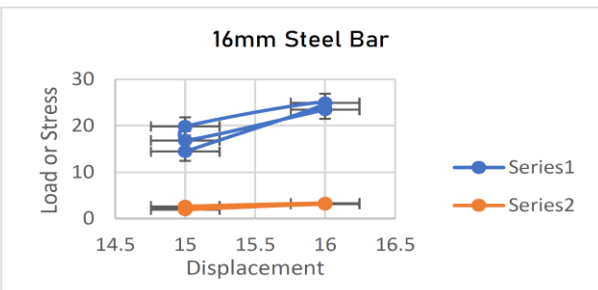

Figure 11. Load-displacement curve of 16mm Steel Bar

3.3. Multiple Regression

As indicated in Table 3, an approximate 70.5% variance score was acquired in the analysis, implying that the model is reliable in predicting the bond strength based on the two predictors: bar diameter and reinforcement type. It is also supported by the acquired Adjusted R square of 67.02%, which shows that the accuracy is still fair, given a more conservative consideration. Likewise, a correspondingly high correlation coefficient of 0.839 further suggests that the Bond strength relationship with the two dependent variables is positively linear.

Table 3. Multiple Regression Statistics

Regression Statistics	
Multiple R	0.839617
R Square	0.704956
Adjusted R Square	0.670245
Standard Error	0.484013
Observations	20

The ANOVA then exhibits the overall significance of the model, resulting in larger regression values than residuals shown in Table 4, indicating that the model covered more of the variation than the unexplained variability.

Table 4. Analysis of Variance

	df	*SS*	*MS*	*F*	*Significance F*
Regression	2	9.515	4.757	20.309	3.12E-05
Residual	17	3.982	0.234		
Total	19	13.498			

Most notably, the regression model is statistically significant given that the p-values of reinforcement type and bar diameter in Table 5 resulted in less than 0.05, wherein the negative coefficient in the reinforcement type illustrates that switching from steel rebars to GFRP bars reduces the bond strength by 17.404%. Meanwhile, in the bar diameter parameter, the negative coefficient infers that the bond strength decreases by about 4.174% for every unit increase in bar diameter. Thus, it is predicted that there is an inverse relationship between the two; the larger the diameter of the bar, the weaker the reinforcement-concrete bond.

Table 5. Regression Coefficients

	Intercept	Reinforcement Type	Bar Diameter
Coefficients	8.25495	-1.4368	-0.34458
Standard Error	0.772907	0.306117	0.054114
t Stat	10.68039	-4.69363	-6.36754
P-Value	5.85E-09	0.000209	7.01E-06
Lower 95%	6.624259	-2.08265	-0.45875
Upper 95%	9.885641	-0.79095	-0.2304
Lower 95.0%	6.624259	-2.08265	-0.45875
Upper 95.0%	9.885641	-0.79095	-0.2304

Moreover, Figure 12.1 shows that the assumptions of linearity and homogeneity of variances are met. This demonstrates that the model is suitable for interpreting the effect of two independent variables on identifying bond strength, given a stable variance indicating an unskewed result. Figure 12.2 then exhibits a normal distribution, provided that the residuals are positioned closely around the slope, validating the hypothesis testing and estimation of the confidence interval, while Figure 12.3 shows two prominent outliers: specimen SB 16-1 and SB 12-2. SB 16-1 presented a relatively low bond strength compared to the other samples of the same type (16 mm steel rebar), which is too low compared to the predicted value. In contrast, SB 12-2 possesses the latter, obtaining a significantly higher bond strength than the model's prediction.

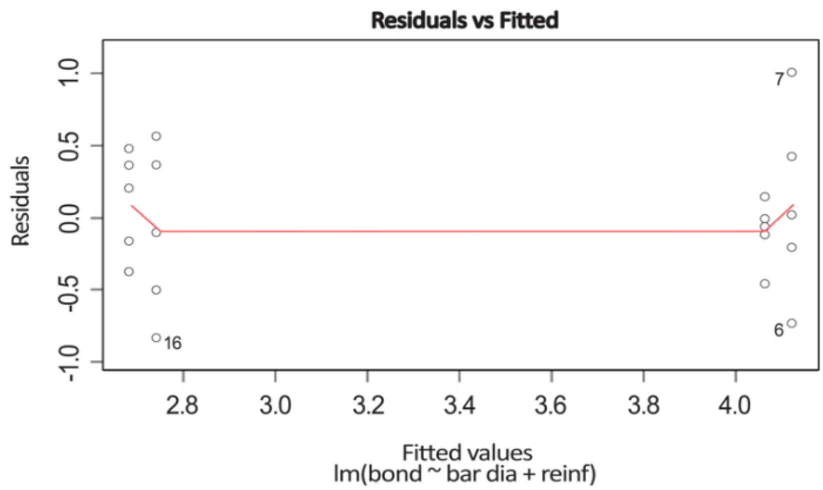

Figure 12.1. Residuals vs. Fitted Plot

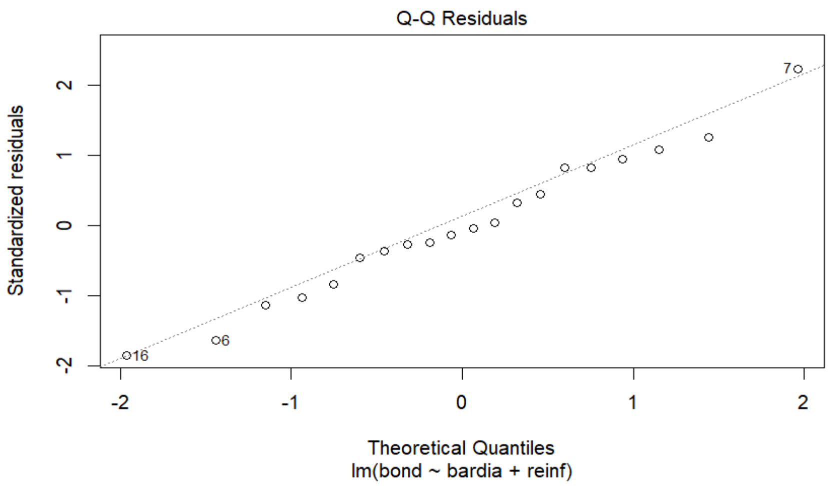

Figure 12.2. Q-Q Plot of Residuals

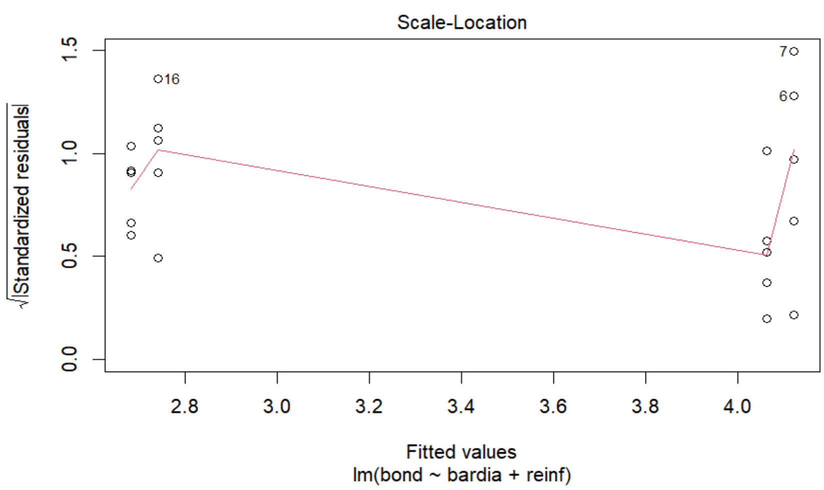

Figure 12.3. Scale-Location Plot

3.4. Effect of Bar Diameter and Reinforcement Type

According to the results exhibited in Figure 13, the GFRP bars with 8mm diameter had been considered to have the most accurate bond strength compared to the other diameters of rebars, regardless of their type. Given that it had the lowest reduction rate of dispersed mean, it leaves the 12mm (GFRP & Steel) and 16mm steel at their high variances of mean bond strength. This means that out of the three diameters used, the 8mm attained the least dispersed bond strength values, making it suitable for the sample used. Moreover, the bond strengths of steel rebars in GFRP at 8mm diameter were significantly higher than those of 16mm steel bars. However, in terms of the 12mm steel, it is observed that it has a higher bond strength mean than the said 8mm GFRP. On the other hand, between the error plots of 8mm GFRP and 12mm steel, the metal rebar had a higher error plot. Hence, in terms of their behavior during pullout, the GFRP behaves better despite crushing the concrete and keeping the rebar intact. In line with this, GFRP rebars have been considered vastly abraded, indicating that the bond strength between the GFRP and concrete was more inclined to shear resistance.

When comparing the two reinforcements of the same diameter (12 mm), on average, Table 6 indicates that 12 mm steel outperforms the 12 mm GFRP bar.

Also, in Table 7, given that it obtained a p-value of 0.00257, which is less than 0.05, the null hypothesis is rejected, implying a significant difference between the performance of steel and GFRP bars having the same bar diameter.

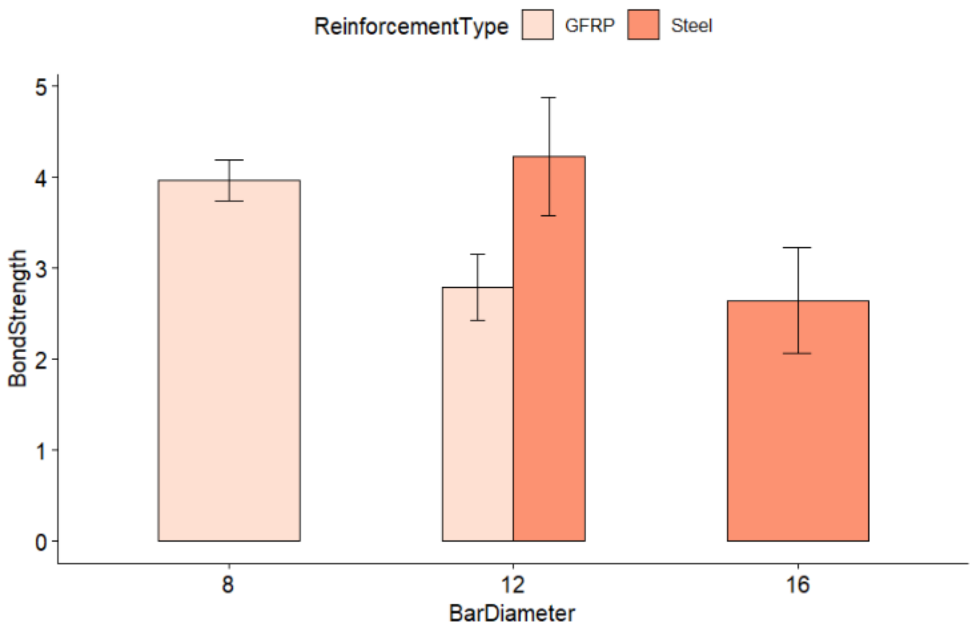

Figure 13. Effect of rebar diameter and reinforcement type on bond strength

Table 6. Descriptive Statistics of 12mm steel and GFRP bar

Groups	Count	Sum	Average	Variance
SB 12	5	21.11	4.222	0.425254
GB 12	5	13.926	2.7852	0.129686

Table 7. ANOVA Summary of 12 mm steel and GFRP bar

Source of Variation	SS	Df	MS	F	P-Value	F-crit
Between Groups	5.1609	1	5.1609	18.603	0.00257	5.3176
Within Groups	2.2193	8	0.277			
Total	7.3803	9				

4. Conclusions

Glass Fiber Reinforced Polymer or GFRP bars are considered a viable alternative to traditional steel reinforcement due to its several beneficial properties. Their corrosion resistance is one of the most appealing characteristics of GFRP bars as it ensures longevity and reduced maintenance in harsh environments where steel reinforcement may suffer in the deterioration. Beyond their corrosion resistance, one of the most notable properties of GFRP bar is their high tensile strength. Despite being lighter than other reinforcement bars, it offers a tensile strength that is comparable to or even exceeds the conventional reinforcement. This tensile strength allows the GFRP reinforcement to support various loads while maintaining structural integrity.

In order to establish that the GFRP bars can be used as an alternative to traditional steel reinforcement, a comprehensive experimental study was conducted to evaluate the bond strength between the uncoated GFRP bars and concrete. This study aims to address the gap in understanding how GFRP bars perform under static loading conditions compared to steel reinforcement. Through experimental data and statistical treatments, the following conclusions were gathered:

1. The bond strength of GFRP bars was found to be lower than traditional reinforcement. The findings highlighted that 17.404% decrease in bond strength happens because of switching from steel reinforcement to GFRP bars. This reduction highlights the need for careful consideration when selecting reinforcement materials, especially when high bond strength application is critical.
2. This study also found that smaller diameter shows higher bond strength than larger diameter, with 8mm GFRP showed the most consistent bond strength. This consistency can be attributed to smaller diameter which increases the bond strength per unit length and the frictional resistance between the bar and concrete. Given the same compressive strength, as the diameter increases, it has a negative effect on bond strength. However, because of the small contact area, the stresses concentrate in a narrower zone of concrete, making the bar more prone to split failure rather than a gradual pull-out.
3. The results of regression analysis showed that both reinforcement type and diameter are statistically significant indicators of bond strength. The R-squared value and F- Statistic suggest that the model explains a substantial portion of the variance in bond strength. Hence, it indicates that these two factors are the key determinants of bond strength in reinforced concrete.
4. In terms of the bond strength of two different reinforcements having the same diameter, it shows that there is a significant difference between the GFRP bars and steel bars. This significant difference suggests that the steel reinforcement still exhibits higher bond strength than GFRP bars when both have the same diameter.
5. The lower displacement values for GFRP bars suggests that they fail by causing localized concrete cracking rather than being pulled out of the concrete. However, despite not achieving the same bond strength as steel, GFRP bars still have the ability to maintain structural integrity without excessive displacement.
6. Lastly, GFRP bars may not match the bond strength of traditional steel reinforcement, its innate ability to withstand corrosion, high tensile strength, and lightweight nature provide distinct advantages that make them a valuable alternative to such applications.

Moreover, it is recommended for future research to consider exploring the ways to improve the bond strength between GFRP bars and concrete. This may involve applying surface treatments, or modifying concrete mixture that will enhance the adhesion of the materials. In this study, uncoated GFRP and traditional concrete mix were used, but different materials may provide additional benefits in certain applications. Additionally, it is important to investigate long-term performance of GFRP bars in order to understand how they behave in different conditions. This will include exposing it to moisture, chemicals, and sunlight for a period of time.

It is also necessary to examine reinforcement samples that have the same diameter in order to accurately compare the bond strength between different materials, such as GFRP bars and steel. This approach will eliminate variability due to geometric differences and provide a clearer understanding into the inherent bond characteristics of each material. Incorporating predictive modeling techniques may also improve the reliability of analyses and support the optimization of reinforcement design. Lastly, examining the mechanical properties of GFRP bars under various loading conditions and testing methods would help build a more comprehensive understanding of their structural performance.

REFERENCES

[1] McCormac, J. C., "Compatibility of Concrete and Steel" in Design of Reinforced Concrete, 10th ed, Wiley US, 2015, p. 6.

[2] Dacuan, C., Abellana, V., "Bond Deterioration of Corroded-Damaged Reinforced Concrete Structures Exposed to Severe Aggressive Marine Environment," International Journal of Corrosion 2021, March 2, pp. 1–13. https://doi.org/10.1155/2021/8847716.

[3] Moodi, Y., Sohrabi, M. R., Mousavi, S. R., "Corrosion effect of the main rebar and stirrups on the bond strength of RC beams" in Structures, vol. 32, pp. 1444-1454, 2021.

https://doi.org/10.1016/j.istruc.2021.03.096.

[4] Jabbar, S. A., Farid, S. B. H., “Replacement of steel rebars by GFRP rebars in the concrete structures” in Karbala International Journal of Modern Science, vol. 4, no.2, pp. 216–227, 2018. https://doi.org/10.1016/j.kijoms.2018.02.002.

[5] Naha, A., Islam, G.M.S., “Bond Strength of Epoxy-Coated Reinforcement in Concrete,” International Conference on Planning, Architecture & Civil Engineering, Rajshahi, Bangladesh, 2021.

[6] Kim, K.-H.E., Andrawes, B. “Behavior of Epoxy-Coated Textured Reinforcing Bars,” Illinois Center for Transportation, no. 18-005, 2018. https://doi.org/10.36501/0197-9191/18-005.

[7] Roman-Liu, Danuta. “Comparison of Concepts in Easy-to-use Methods for MSD Risk Assessment,” Applied Ergonomics, vol. 45, no. 3, pp. 420–427, 2013. https://doi.org/10.1016/j.apergo.2013.05.010.

[8] Zheng, X., Du, H., Zhang, R., Ma, Q., Gao, H. “Static load test of RC T-Beam Bridge flexural strengthening with externally bonded steel plates,” 2021 3rd International Conference on Advances in Civil Engineering, Energy Resources and Environment Engineering, Qingdao, China, May 28-30. https://doi.org/10.1088/1755-1315/791/1/012018.

[9] Laskar, S. M., Mozumder, R. A., Laskar, A. I., “Behaviour of RC beam repaired using alkali activated slag-based agent under static and cyclic loading” in Structures, vol. 31, pp. 761–768, 2021. https://doi.org/10.1016/j.istruc.2021.02.039.

[10] Abbadi, A., Basheer, P., Forth, J. P., “Effect of hybrid fibres on the static load performance of concrete beams” in Materials Today: Proceedings, vol. 65, pp. 681–687, 2022. https://doi.org/10.1016/j.matpr.2022.03.263.

[11] Fuchs, W., Hofmann, J., “Post-installed reinforcing bars – requirements for their reliable use” in Developments in the Built Environment, vol. 5, 2021. https://doi.org/10.1016/j.dibe.2020.100040.